Cytoplasmic carboxypeptidase 5 regulates tubulin glutamylation and zebrafish cilia formation and function

Narendra Pathak[a], Christina A. Austin-Tse[b,*], Yan Liu[a,†], Aleksandr Vasilyev[c,‡], and Iain A. Drummond[a,b]
[a]Nephrology Division and [c]Department of Pathology, Massachusetts General Hospital, Charlestown, MA 02129;
[b]Department of Genetics, Harvard Medical School, Boston, MA 02115

ABSTRACT **Glutamylation is a functionally important tubulin posttranslational modification enriched on stable microtubules of neuronal axons, mitotic spindles, centrioles, and cilia. In vertebrates, balanced activities of tubulin glutamyl ligase and cytoplasmic carboxypeptidase deglutamylase enzymes maintain organelle- and cell type–specific tubulin glutamylation patterns. Tubulin glutamylation in cilia is regulated via restricted subcellular localization or expression of tubulin glutamyl ligases (*ttlls*) and nonenzymatic proteins, including the zebrafish TPR repeat protein Fleer/Ift70. Here we analyze the expression patterns of *ccp* deglutamylase genes during zebrafish development and the effects of *ccp* gene knockdown on cilia formation, morphology, and tubulin glutamylation. The deglutamylases *ccp2*, *ccp5*, and *ccp6* are expressed in ciliated cells, whereas *ccp1* expression is restricted to the nervous system. Only *ccp5* knockdown increases cilia tubulin glutamylation, induces ciliopathy phenotypes, including axis curvature, hydrocephalus, and pronephric cysts, and disrupts multicilia motility, suggesting that Ccp5 is the principal tubulin deglutamylase that maintains functional levels of cilia tubulin glutamylation. The ability of *ccp5* knockdown to restore cilia tubulin glutamylation in *fleer/ift70* mutants and rescue pronephric multicilia formation in both *fleer*- and *ift88*-deficient zebrafish indicates that tubulin glutamylation is a key driver of ciliogenesis.**

Monitoring Editor
Stephen Doxsey
University of Massachusetts

Received: Jan 14, 2013
Revised: Apr 2, 2014
Accepted: Apr 7, 2014

INTRODUCTION

Glutamylation is an evolutionarily conserved posttranslational modification that occurs prominently on α- and β-tubulin associated with stable microtubules of mitotic spindles, neuronal axons, centrioles, and cilia (Edde *et al.*, 1990). Functionally, tubulin glutamylation regulates cytoskeletal processes by modulating microtubule–protein interactions, such as those with neuronal kinesin motor KIF-1A during neurite extension (Ikegami *et al.*, 2007) and with septins during polarized vesicle transport (Spiliotis *et al.*, 2008). In addition, glutamylation stimulates the activity of the microtubule-severing protein spastin during microtubule disassembly (Lacroix *et al.*, 2010) and modulates the activities of inner arm dyneins to regulate cilia motility (Kubo *et al.*, 2010; Suryavanshi *et al.*, 2010). Variations in tubulin glutamylation patterns contribute to the structural and functional heterogeneity of microtubules in distinct organelles of vertebrate organisms (Verhey and Gaertig, 2007). Cytoplasmic microtubules are not glutamylated (Bobinnec *et al.*, 1998), whereas cilia transition zone microtubules are monoglutamylated, and neuronal and axonemal microtubules are polyglutamylated (Edde *et al.*, 1991; Fouquet *et al.*, 1994; Huitorel *et al.*, 2002; Kann *et al.*, 2003). Biochemically, glutamylation is a reversible process. Glutamate side chains are linked to genetically encoded glutamate(s) within C-termini of α- or β-tubulin by tubulin glutamyl ligase members of the tubulin tyrosine ligase–like (TTLL) protein family (Janke *et al.*, 2005; van Dijk *et al.*, 2007). Conversely, side chain glutamates are removed by tubulin deglutamylase members of the cytoplasmic carboxy peptidase (CCP) protein family (Rogowski *et al.*, 2010). It is believed that

This article was published online ahead of print in MBoC in Press (http://www.molbiolcell.org/cgi/doi/10.1091/mbc.E13-01-0033) on April 17, 2014.

Present addresses: *Journal of Visualized Experiments, 1 Alewife Center, Suite 200, Cambridge, MA 02140; †Fred Hutchinson Cancer Research Center, 1100 Fairview Ave. N., Seattle, WA 98109; ‡NYIT-College of Osteopathic Medicine, Old Westbury, NY 11568

N.P., A.V., and I.A.D. designed the experiments; N.P. performed the experiments, with the exception of electron microscopy, which was performed by C.A.A.

Address correspondence to: Narendra Pathak (NPATHAK@mgh.harvard.edu).

Abbreviations used: CCP, cytoplasmic carboxy peptidase; TTLL, tubulin tyrosine ligase like.

the diversity of microtubule subtypes generated by tubulin post-translational modifications is maintained by balanced activities of TTLL glutamylases and CCP deglutamylases; however, the functional repertoire of *ttll* and *ccp* genes in different organisms is not fully known.

The protein localization and expression patterns of vertebrate tubulin glutamyl ligases and deglutamylases suggest unique roles for different *ttll* or *ccp* gene family members (Pathak *et al.*, 2011; Bosch Grau *et al.*, 2013; Lyons *et al.*, 2013). Green fluorescent protein (GFP) fusion proteins of TTLL1, TTLL9, and TTLL11 show preferential localization to cilia basal bodies, whereas those of TTLL5, TTLL6, and TTLL7 localize along ciliary axonemes (Janke *et al.*, 2005; van Dijk *et al.*, 2007). Functional studies reveal that TTLL1 is required for respiratory cilia and sperm motility (Ikegami *et al.*, 2010; Vogel *et al.*, 2010), whereas TTLL5 is exclusively required for sperm motility (Lee *et al.*, 2013). Analysis of *ttll* mRNA expression in developing zebrafish and mouse brain ependymal cells suggests that *ttll6* is uniquely important in ciliated cells, whereas *ttll1*, *ttll4*, and *ttll7* may function in both ciliated cells and neurons (Pathak *et al.*, 2011; Bosch Grau *et al.*, 2013). *ttll6* knockdown in zebrafish embryos or cultured ependymal cells primarily affects cilia motility (Pathak *et al.*, 2011; Bosch Grau *et al.*, 2013), whereas *ttll1* is required for glutamylation of zebrafish secondary motor neurons (Pathak *et al.*, 2011) and TTLL7 is required for growth of MAP2-positive neurites in PC12 cells (Ikegami *et al.*, 2006).

Tubulin deglutamylases also play important roles in cilia and neurons. In *Caenorhabditis elegans*, GFP fusion proteins of the tubulin deglutamylases CCPP-1 and CCPP-6 localize to amphid cilia (Kimura *et al.*, 2010; O'Hagan *et al.*, 2011). Mutation in *C. elegans* ccpp-1 causes excessive accumulation of KLP-6 kinesin and polycystin-2 in cilia and also increases the transport rate of OSM-3/KIF17 on axonemal microtubules (Kimura *et al.*, 2010; O'Hagan *et al.*, 2011). Deficiency of the mouse CCP1 tubulin deglutamylase increases polyglutamylation of brain neurons in *pcd* mice, leading to their progressive degeneration (Fernandez-Gonzalez *et al.*, 2002; Rogowski *et al.*, 2010). In zebrafish, whole-embryo quantitative PCR studies show that *ccp1, ccp2, ccp5,* and *ccp6* mRNA expression increases over the first 8 d of development; however, the tissue-specific expression of zebrafish *ccp* genes and how expression correlates with *ccp* gene function have not been fully explored (Lyons *et al.*, 2013).

In addition to changes in glutamylase and deglutamylase activity, tubulin glutamylation can be altered by mutations in putative basal body and intraflagellar transport (IFT)–associated proteins. Mutation in human *CEP41* results in loss of cilia, aberrant TTLL6 localization, and consequent reduction in axonemal tubulin glutamylation (Lee *et al.*, 2012). Mutation in the zebrafish *fleer/ift70* gene causes significant reduction in axonemal tubulin glutamylation and loss of multiciliated cell ciliogenesis (Pathak *et al.*, 2007). Fleer/Ift70 is a tetratrico peptide repeat (TPR)–rich protein related to CeDYF-1/CrIft-70 and is a component of the IFT complex (Fan *et al.*, 2010). It is not known whether *fleer* mutants lack tubulin glutamyl ligase activity or mislocalize Ttll enzymes, or, alternatively, whether the Fleer protein limits the activity of deglutamylases or restricts their access to the cilia compartment.

Here we focus on the expression and function of zebrafish *ccp* deglutamylases in normal and *fleer*- or *ift88*-deficient cilia. We find that expression of zebrafish *ccp* deglutamylase genes *ccp2*, *ccp5*, and *ccp6* is strongly enriched in ciliated cell types, whereas *ccp1* expression is restricted to the nervous system and somites. Despite overlapping expression patterns, we find that *ccp5* is the major deglutamylase in zebrafish cilia and that *ccp5* deficiency can restore cilia glutamylation in the *fleer* mutant and improve multiciliogenesis in *fleer*- and *ift88*-deficient zebrafish.

RESULTS

Expression of tubulin deglutamylases during zebrafish development

Tubulin deglutamylases are members of the M14 CCP protein family, alternatively known as ATP/GTP-binding protein–like family. Zebrafish harbor four orthologues of mouse deglutamylase genes: *Ccp1*, *Ccp2*, *Ccp5*, and *Ccp6* (Supplemental Figure S3A; Lyons *et al.*, 2013). A limited analysis of zebrafish *ccp* gene expression found evidence for specific expression of *ccp1*, *ccp2*, and *ccp5* in the pronephros and olfactory placode (Lyons *et al.*, 2013). We undertook a complete expression analysis of *ccp1*, *ccp2*, *ccp5*, and *ccp6* and found that *ccp1* expression was confined mainly to the developing CNS and somites at all developmental stages, whereas *ccp2*, *ccp5*, and *ccp6* were highly expressed in multiple ciliated cell types, including Kupffer's vesicle (KV), nephrogenic mesoderm, the pronephros, otic placode, olfactory placode, and lateral line organs (Figure 1 and Supplemental Figure S1). *ccp1* and *ccp5* were maternally expressed in four- to eight-cell-stage embryos (Figure 1, A and C). At the 10-somite stage, *ccp1* was expressed on the periphery of KV and in axial neurogenic cells (Figure 1, E and I), whereas *ccp5* and *ccp6* (Figure 1, G and H) but not *ccp2* (Figure 1F) were expressed in KV epithelial cells. Expression of *ccp2*, *ccp5*, and *ccp6* was also observed in the nephrogenic mesoderm at this stage and persisted until 54 h postfertilization (hpf) (Figure 1, J–L and N–P, and Supplemental Figure S1, F–H and J–L), whereas *ccp1* expression continued to be restricted to brain and spinal cord (Figure 1, M and Q). At 54 hpf, *ccp2*, *ccp5*, and *ccp6* were all expressed in the olfactory placode (Figure 1, R–T), while *ccp6* was also expressed in the retina and otic placode (Figure 1T). Overall the expression patterns of *ccp2*, *ccp5*, and *ccp6* show enrichment in ciliated cells, similar to the glutamyl ligase gene *ttll6* and the glutamylation regulator *fleer* (Pathak *et al.*, 2007, 2011).

ccp5 knockdown induces ciliopathy phenotypes

To assess the function of *ccp* genes in ciliogenesis, we knocked down *ccp1*, *ccp2*, *ccp5*, and *ccp6* using antisense morpholinos. Injections of splice-blocking morpholino oligos caused near-complete elimination of wild-type *ccp* gene mRNA (Figure 2A and Supplemental Figure S2A), resulting in truncated splice products predicted to encode proteins lacking carboxypeptidase domains (Supplemental Figure S3, B–F). Of these four genes, only *ccp5* knockdown induced a typical spectrum of ciliopathy phenotypes, including axis curvature, pronephric cysts, and hydrocephalus (Figure 2B). Whereas isolated hydrocephalus was observed in *ccp1* morphants (Figure 2, B and C), this was accounted for by widespread cell death in the CNS (Supplemental Figure S2B), similar to the CCP1-deficient mouse *pcd* mutant phenotype (Mullen *et al.*, 1976; Rogowski *et al.*, 2010), with subsequent obstruction of the spinal canal with cell debris (Supplemental Figure S2B). Although knockdown of *ccp2* eliminated all wild-type *ccp2* mRNA, no obvious embryonic phenotype was frequently observed (Supplemental Figure S2, A and B).

ccp5 deficiency induces cilia microtubule hyperglutamylation and motility defects

To determine the cellular basis of ciliopathy phenotypes in *ccp5*-deficient embryos, we analyzed cilia in the pronephros and brain ventricles with respect to glutamylated tubulin content, length, and motility. Double immunolabeling of whole-mount embryos with monoclonal antibody (mAb) GT335 (recognizing monoglutamylated

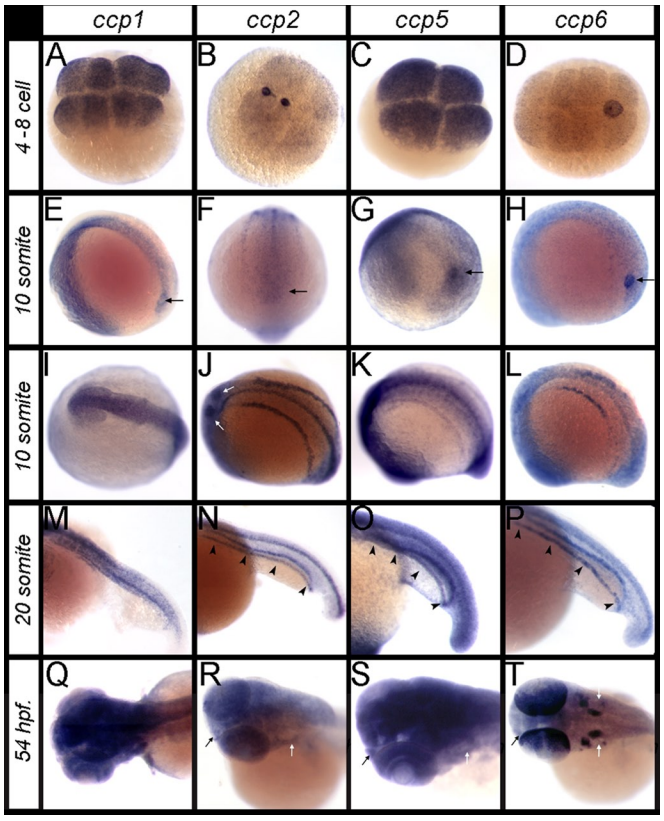

FIGURE 1: RNA in situ hybridization patterns of *ccp1*, *ccp2*, *ccp5*, and *ccp6* during zebrafish development. (A–D) The four- to eight-cell-stage embryos, showing maternal transcripts of (A) *ccp1*, (B) *ccp2*, (C) *ccp5*, and (D) *ccp6*. (E–H) Lateral and caudal views of 10-somite embryos, showing expression of (E) *ccp1*, (F) *ccp2*, (G) *ccp5*, and (H) *ccp6* relative to the Kupffer's vesicle (black arrows). (I–L) Dorsal views of 10-somite embryos, showing expression of (I) *ccp1* in the CNS and (J) *ccp2*, (K) *ccp5*, and (L) *ccp6* in the spinal canal and bilateral nephrogenic mesoderm. (M–P) Twenty-somite embryos, showing that (M) *ccp1* is expressed medially in somites and spinal canal, whereas (N) *ccp2*, (O) *ccp*5, and (P) *ccp6* expression is prominent medially in the spinal canal and bilaterally in the pronephroi (black arrowheads). (Q–T) Dorsal views of the head in 54-hpf larvae, showing (Q) *ccp1*, (R) *ccp2*, (S) *ccp5*, and (T) *ccp6* are widely expressed in CNS, eye, otic placode (white arrows), and olfactory placode (black arrows). In T, note the distinct expression of *ccp6* in otic placodes and posterior cell layers of the eye.

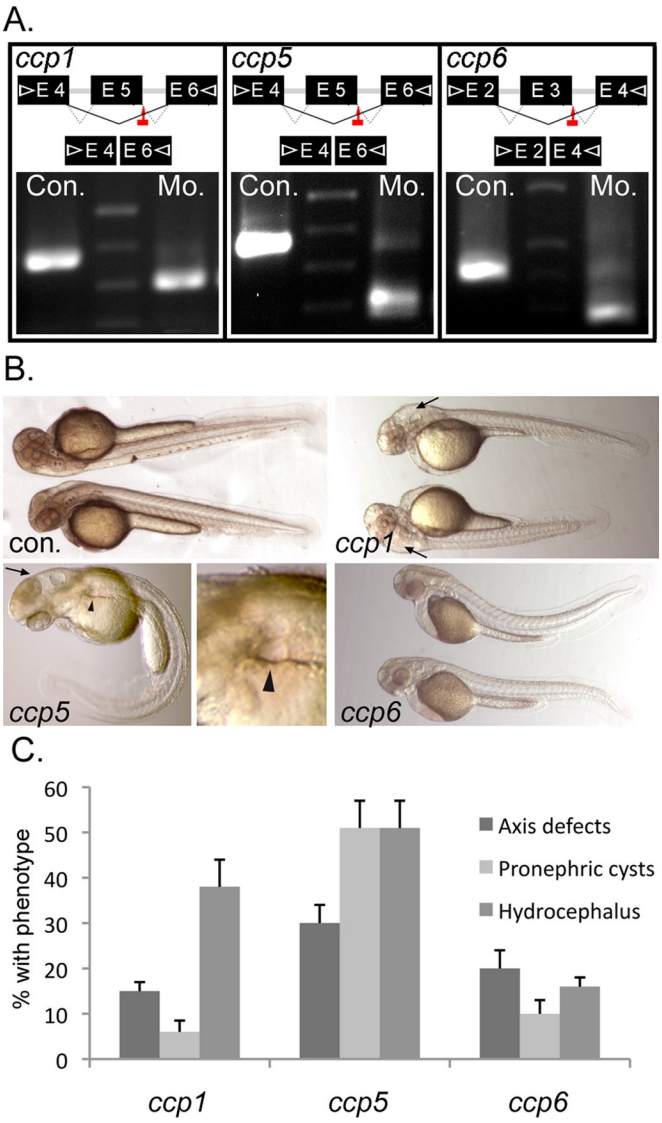

FIGURE 2: *ccp5* knockdown alone induces the typical spectrum of ciliopathy phenotypes in wild-type zebrafish. (A) Splice donor sites targeted by antisense morpholinos (red arrows) in *ccp1*, *ccp5*, and *ccp6* genes and agarose gel analysis showing RT-PCR amplicons of *ccp1*, *ccp5*, and *ccp6* generated using primer pairs (arrowheads) in indicated exons were smaller in morphant (Mo.) embryos than in respective control (Con.) In each case, the reduced size of morphant amplicon relative to control matched the size of the deleted target exon. (B) External morphology of 2.5-d-old zebrafish injected with optimal dose of control or antisense morpholinos designed to knock down *ccp1*, *ccp5*, and *ccp6* genes, respectively. (C) Frequency of phenotype associated with cilia defects. *ccp1* morphants mostly exhibit isolated hydrocephalus, whereas *ccp5* morphants exhibit hydrocephalus and pronephric cysts, often with acutely curved body axis. Replicates: *ccp1×5Mo* ($n = 181$ embryos/4 injections); *ccp5×5Mo* ($n = 275$ embryos/5 injections); *ccp6×3Mo* ($n = 261$embryos/5 injections).

or polyglutamylated tubulin) and mAb 6-11B-1 (specific to acetylated tubulin) allowed direct assessment of cilia tubulin glutamylation in wild-type versus *ccp5*-deficient embryos (Figure 3). Tubulin glutamylation in control single cilia and multicilia extends along the length of the cilium (Figure 3, A and C, and Supplemental Figure S4, A and C; also see later discussions of Figures 5, A and C, and 6), decreasing from the base to the tip (Pathak *et al.*, 2007). Relative to control cilia imaged under identical conditions, glutamylated tubulin immunoreactivity was significantly increased relative to acetylated tubulin in *ccp5*-deficient cilia (Figure 3, D–F, and later discussions of Figures 5, D–F, and 6), whereas it appeared unchanged in cilia of *ccp1* (unpublished data) and *ccp6* morphants (Figure 3, G–I). Measurements of the axonemal extent of immunolabeling of single pronephric cilia for glutamylated versus acetylated tubulin revealed a small but significant increase in the extent of tubulin glutamylation in *ccp5*-deficient cilia (Figure 3J), whereas overall cilia length (acetylated tubulin) was not significantly different. To quantify tubulin glutamylation in cilia, we acquired multiple images of immunolabeled multicilia under identical conditions and analyzed them using ImageJ to measure total pixel intensity for red (glutamylated tubulin) and green (acetylated tubulin) channels in the same region of interest. Expressing the intensity of the red and green channels as a ratio, we found that pronephric cilia tubulin glutamylation increased

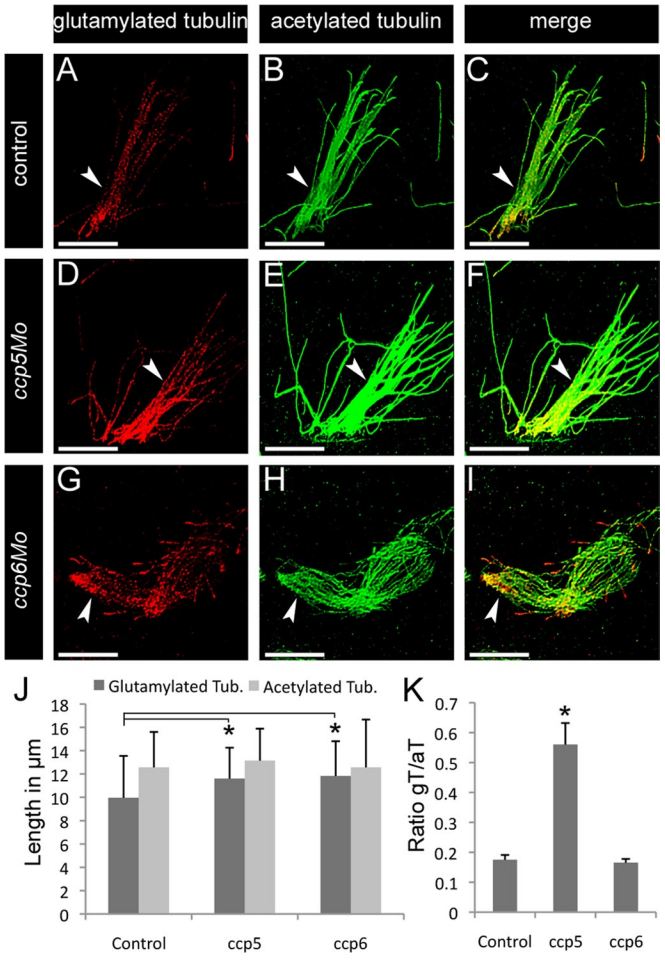

FIGURE 3: *ccp5* knockdown induced hyperglutamylation of cilia microtubules. Representative images of pronephric cilia from 2.5-d-old zebrafish larvae double immunolabeled with glutamylated tubulin–specific mAb GT335 (red) and acetylated tubulin–specific mAb 6-11B-1 (green), Scale bars, 10 µm. (A–C) Pronephric multicilia (arrowheads) from control larva showing that (A) glutamylated tubulin normally decreases from the base to the tip of axonemes, in contrast to (B) uniformly distributed acetylated tubulin. (D–F) Pronephric multicilia from *ccp5* morphant larva showing (D) enhanced labeling intensity of glutamylated tubulin along their axonemes marked by (E) acetylated tubulin. (G–I) Pronephric multicilia from *ccp6* morphant, showing that (G) labeling intensity of glutamylated tubulin along their axonemes marked by (H) acetylated tubulin is similar to control. (J) Average length of glutamylated tubulin labeled segment increased in the pronephric cilia of *ccp5* and *ccp6* morphants relative to controls, although length of their acetylated tubulin-labeled segments was similar. Control ($n = 33$, cilia/4 larvae), *ccp5* morphants ($n = 42$ cilia/4 larvae), *ccp6* morphants ($n = 31$ cilia/4 larvae). Error bars, SD; *t* test, $*p < 0.05$. (K) Average intensity ratio of glutamylated tubulin relative to acetylated tubulin significantly increased in pronephric cilia of *ccp5* morphants relative to control or *ccp6* morphants. n = 36 cilia/4 control larvae; 33 cilia/4 *ccp5* morphant larvae; 45 cilia/4 *ccp6* morphant larvae. Error bars, SEM; *t* test, $*p < 0.05$.

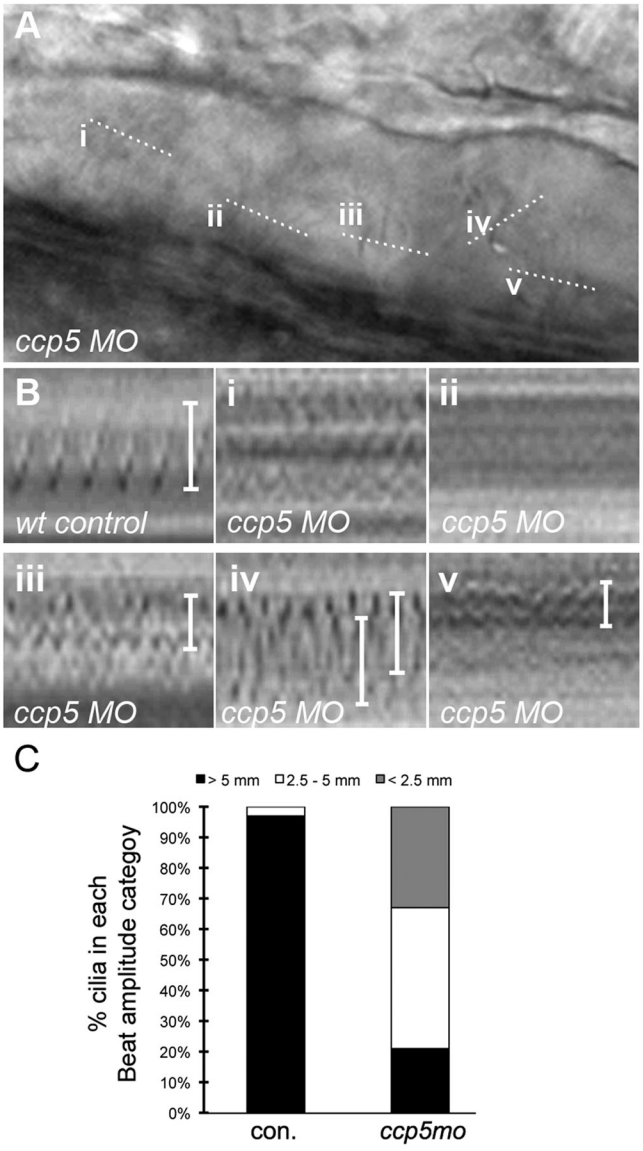

FIGURE 4: *ccp5* inactivation perturbs cilia motility. (A) Frame of a movie taken of pronephric cilia from a 2.5-d-old *ccp5* morphant. Lower-case Roman numerals indicate multicilia analyzed for motility defects; dotted lines indicate the plane of the line scanned through the cilium. (B) Kymograms of pronephric cilia from a wild-type control and *ccp5*-deficient multicilia (i–v) from the movie frame in A. (C) Quantitative representation of beat amplitude categories of pronephric multicilia observed in control embryos ($n = 36$ cilia from eight embryos) and *ccp5* morphants ($n = 33$ cilia from seven embryos).

2.5-fold (0.56) in *ccp5*-deficient cilia compared with control (0.20; Figure 3K), whereas the average ratio of glutamylated tubulin to acetylated tubulin in *ccp6*-deficient cilia was similar to control (0.165). High-speed videomicroscopy analysis of pronephric multicilia motility from 2.5-d-old control larvae revealed a synchronous waveform with an average beat amplitude of 6 µm (Figure 4, B and C, and Supplemental Movie S1). In contrast, motile multicilia in the *ccp5*-deficient morphants were uncoordinated with individual *ccp5*-deficient cilia either completely paralyzed or moving independently with significantly reduced beat amplitudes (Figure 4, B and C, and Supplemental Movie S2). Cilia tubulin hyperglutamylation thus appears to inhibit motility-associated functions of microtubules.

ccp5 knockdown restores tubulin glutamylation and promotes multicilia assembly in IFT-deficient zebrafish

We previously showed that mutation in the zebrafish cilia TPR protein Fleer/Ift70 significantly reduced axonemal tubulin

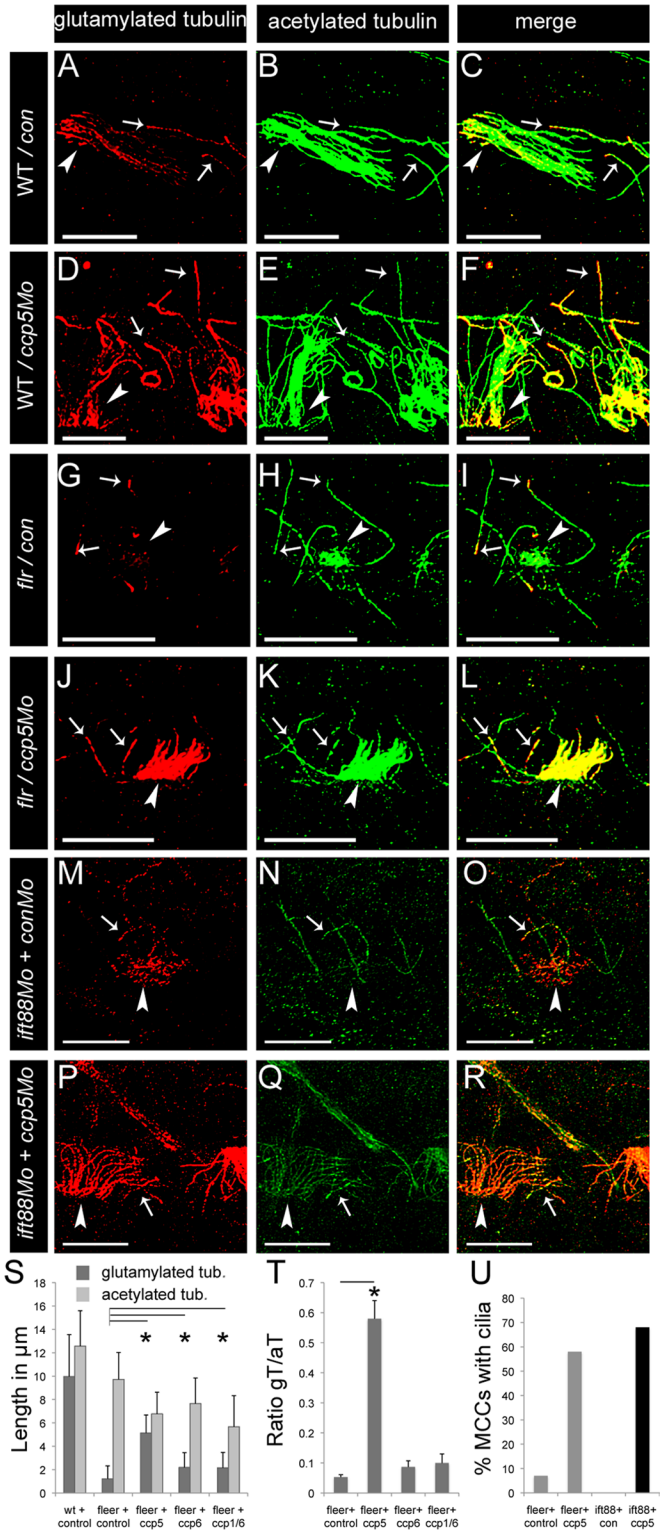

FIGURE 5: *ccp5* knockdown in Fleer- and Ift88-deficient zebrafish promotes pronephric multicilia assembly. (A–R) Representative images of pronephric single cilia (white arrows) and multicilia (white arrowheads) of 2.5-d-old zebrafish larvae double immunolabeled with glutamylated tubulin–specific mAb GT335 (red) and acetylated tubulin–specific mAb 6-11B-1 (green). Scale bars, 10 µm. (A–C) Pronephric cilia in control larva showing (A) that glutamylated tubulin levels gradually decrease from base to tip of axonemes; (B) that acetylated tubulin is uniformly distributed along the entire length of axonemes; and (C) their merge. (D–F) Pronephric cilia in *ccp5* morphant showing (D) glutamylated tubulin at elevated levels along the entire length of axonemes, (E) acetylated tubulin, and (F) their merge. (G–I) Pronephric cilia of *fleer* mutant injected with control morpholino showing (G) glutamylated tubulin restricted near the base of single cilia and absent in multicilia, (H) acetylated tubulin in axonemes of single cilia and accumulated in cytoplasm of multiciliated cells, and (I) their merge. (J–L) Pronephric cilia of *fleer* mutant injected with *ccp5×5Mo* showing (J) glutamylated tubulin at elevated levels in axonemes of both single and multicilia, (K) acetylated tubulin in axonemes of single cilia and restored multicilia (note reduced cytoplasmic accumulation of acetylated tubulin in multiciliated cells), and (L) their merge. (M–O) Pronephric cilia of *ift88* morphants showing (M) glutamylated tubulin gradually decreasing along single cilia and abnormally accumulated at the base of multicilia, (N) acetylated tubulin present along single cilia but notably absent in multiciliated cells, and (O) their merge. (P–R) Pronephric cilia in double morphant of *ift88* and *ccp5* showing (P) glutamylated tubulin at elevated levels in axonemes of both single and restored multicilia (note reduced cytoplasmic accumulation of glutamylated tubulin in multiciliated cells), (Q) acetylated tubulin in single and restored multicilia, and (R) their merge. (S) Average length of glutamylated tubulin– and acetylated tubulin–labeled segments in pronephric cilia of WT zebrafish injected with control Mo ($n = 33$ cilia/4 larvae), *fleer* mutants injected with control Mo ($n = 50$ cilia/4 larvae), *ccp5×5Mo* ($n = 55$ cilia/5 larvae), *ccp6×3*Mo alone ($n = 60$ cilia/4 larvae), and the combination ccp*1*×5Mo/*ccp6*×3*Mo* ($n = 86$ cilia/5 larvae). Error bars, SD; *t* test, $*p < 0.05$. (T) Average intensity ratios of glutamylated tubulin relative to acetylated tubulin measured in individual double-immunolabeled pronephric single cilia and multicilia from *fleer* mutant larvae injected with control MO ($n = 48$ cilia/4 larvae), *ccp5×5Mo* ($n = 78$ cilia/ 6 larvae), *ccp6×3Mo* alone ($n = 41$ cilia/ 4 larvae), and the combination *ccp1*×5*Mo*/*ccp6*×3*Mo* ($n = 36$ cilia/4 larvae). Error bar, SEM; *t* test, $*p < 0.05$. (U) Percentage of MCCs that extend axonemes >2 µm from their apical surface in the pronephros of *fleer* mutants injected with control morpholino ($n = 55$ MCCs/6 larvae), *fleer* mutants injected with *ccp5×5Mo* ($n = 48$ MCCs/8 larvae), zebrafish injected with the combination *ift88Mo* and control Mo ($n = 43$ MCCs/8 larvae), and zebrafish injected with the combination *ift88Mo* and *ccp5×5Mo* ($n = 41$ MCCs/8 larvae).

glutamylation, cilia motility, and single cilia length and blocked ciliogenesis in multiciliated cells (Pathak *et al.*, 2007). Given the increase in cilia glutamylation we observed with *ccp5* knockdown, we tested whether compound deficiency of *ccp* deglutamylases and *fleer* would restore glutamylation in *fleer* mutant cilia. We injected *fleer*^{ca1} in-cross clutches with control, *ccp5*, *ccp6*, and *ccp1/ccp6* morpholinos and identified homozygous *fleer*$^{ca1-/-}$ 2.5-d-old larvae by genotyping. We then performed double immunolabeling with mAb GT335, specific to glutamylated tubulin, and 6-11B-1, specific to acetylated tubulin. Analysis of glutamylated tubulin in control (Figure 5A) and *fleer* mutant pronephric single cilia (arrows in Figure 5, G and I; Figure 6) confirmed that tubulin glutamylation was significantly reduced and restricted to the cilia base in *fleer* larvae. Multiciliated cells in the *fleer* mutants do not extend axonemes or show glutamylated basal bodies (arrowhead, Figure 5G; Pathak *et al.*, 2007) but instead have aberrant apical cytoplasmic accumulation of acetylated tubulin (arrowhead, Figure 5H; Supplemental Figure S4, E, H, and K, and Figure 6). Strikingly, compound *fleer* mutant/*ccp5* morphants showed significantly increased intensity of glutamylated tubulin reactivity in single cilia and prominent glutamylated tubulin-positive axonemes extending from pronephric multiciliated cells (Figures 5, J–L, and 6). Restoration of glutamylation or multicilia axoneme elongation was not observed in compound *fleer/ccp6* morphants (Supplemental Figure S5, G–I) or *fleer/ccp1/ccp6* morphants

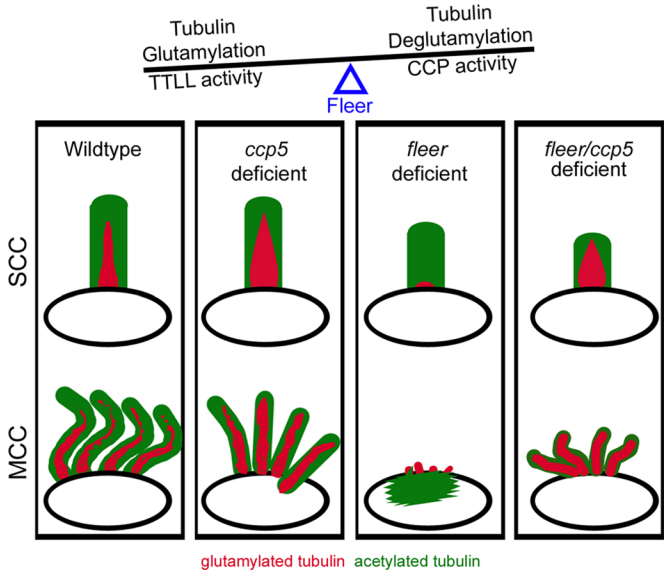

FIGURE 6: Schematic depicting *ccp5* knockdown–induced changes to tubulin glutamylation in normal and *flee*-deficient cilia. In normal cilia of wild-type single ciliated cells (SCCs) and MCCs, glutamylated tubulin is enriched maximally at the base and gradually decreases toward the tip. Loss of *ccp5* in otherwise normal cilia significantly increases the overall amount and extent of glutamylated tubulin without increasing cilia length. Hyperglutamylation inhibits efficient cilia motility. Glutamylated tubulin is significantly reduced and restricted to the base of short, single cilia that persist in the *fleer* mutants. Fleer-deficient cilia remain competent for tubulin glutamylation and show greater-than-normal increase in overall intensity and extent when Ccp5 deglutamylase is knocked down in the *fleer* mutants. Multicilia in *fleer* mutants are more sensitive to the loss of glutamylation; however, multiciliated cells in compound *fleer/ccp5*-deficient zebrafish show improved assembly of cilia upon increase in tubulin glutamylation.

(Supplemental Figure S5, J–L). Quantification of the extent of glutamylated and acetylated tubulin in individual cilia from *fleer* mutant or compound *fleer/ccp*-gene deficient larvae (Supplemental Figure S5) revealed that whereas glutamylated tubulin was confined to an average 1.2 µm length at the base of single cilia in *fleer* mutants, this increased significantly to 5.1 µm in cilia of *fleer/ccp5*-deficient larvae. However, the extent of acetylated tubulin in single pronephric cilia of *ccp5/fleer*-deficient larvae (6.8 µm) was reduced compared with cilia deficient in *fleer* alone (9.7 µm). Compound *fleer/ccp6*- and *fleer/ccp1/ccp6*-deficient larvae did not show a significant restoration of the axonemal extent of glutamylated tubulin reactivity (2.2 µm; Supplemental Figure S5). Assessment of the overall pixel intensity of glutamylated tubulin reactivity relative to acetylated tubulin in the same cilia (Figure 5T) revealed a low intensity ratio for glutamylated:acetylated tubulin in pronephric single cilia of *fleer* (0.05), *fleer/ccp6*-deficient (0.08), and *fleer/ccp1/ccp6*-deficient larvae (0.1) compared with control cilia (0.20). Cilia of *fleer/ccp5*-deficient larvae showed a remarkable recovery in the glutamylated:acetylated tubulin ratio intensity (0.58; Figure 5T). Recovery of tubulin glutamylation in compound *fleer/ccp5* deficient multiciliated cells (MCCs) correlated with reappearance of short apical MCC cilia (Figures 5, J–L and U, and 6), indicating that *ccp5* knockdown could partially rescue *fleer* mutant multiciliogenesis.

To test whether rescue of multiciliogenesis by *ccp5* knockdown was specific to *fleer* mutants, we examined *ift88*-deficient zebrafish that similarly fail to generate cilia on MCCs (Tsujikawa and Malicki, 2004; Kramer-Zucker *et al.*, 2005). In 2.5-d-old *ift88* morphants, pronephric MCCs show glutamylated basal bodies (Figure 5M and Supplemental Figure S5A) but no acetylated tubulin (Figure 5, N and O) or Arl13b-positive cilia (Supplemental Figure S5, B and C). In contrast, in *ift88/ccp5* double morphants, ~70% of pronephric MCCs (Figure 5U) showed axonemes that were strongly labeled by glutamylated tubulin (arrowheads in Figure 5P; Supplemental Figure S5D), acetylated tubulin (Figure 5, Q and R), or Arl13b (Supplemental Figure S5, E and F). Our results demonstrate that cilia in the *fleer* mutant are competent for tubulin glutamylation (Figure 6) and suggest that high levels of tubulin glutamylation generated by *ccp5* knockdown can exert a dominant positive effect on multiciliogenesis, even in cells deficient for Fleer/Ift70 or Ift88.

DISCUSSION

Tubulin glutamylation is an important posttranslational modification that is regulated by the balanced activities of *ttll* tubulin ligases and *ccp* tubulin deglutamylases (Janke and Bulinski, 2011). Our results show that the zebrafish *ccp* gene family is broadly expressed during development and Ccp5 is the key deglutamylase that maintains the functional set-point of cilia tubulin glutamylation. Tubulin glutamylation is also regulated in cilia by the Fleer/Ift70 protein, and we show that *ccp5* knockdown partially overcomes multicilia elongation defects in Fleer/Ift70- and Ift88-deficient zebrafish. Our findings suggest that increased glutamylation can drive initial assembly of multicilia axonemes but that prevention of excessive tubulin glutamylation by *ccp5* deglutamylase activity is essential for mature cilia motility and function.

Zebrafish *ccp* gene expression and function

Our analysis of *ccp* gene expression in zebrafish revealed that all four zebrafish *ccp* genes were expressed throughout embryonic development, extending a previous analysis of *ccp* gene expression in zebrafish (Lyons *et al.*, 2013). Specifically, we find that in addition to *ccp1* and *ccp5*, the tubulin deglutamylase genes *ccp2* and *ccp6* are expressed in multiple ciliated tissues throughout embryogenesis. Although overlapping expression of *ccp2*, *ccp5*, and *ccp6* suggested the possibility of redundant deglutamylating activity in cilia, we found that *ccp5* was the principal enzyme involved in regulating ciliary glutamyl tubulin levels. Previously *ccp5* knockdown was shown by Western blotting to globally increase embryo glutamyl tubulin, but this did not distinguish between cilia and the abundant tubulin glutamylation in brain and spinal cord neurons (Lyons *et al.*, 2013). In addition, in contrast to previous reports, we did not see an increase in cilia tubulin glutamylation in *ccp1*-deficient embryos (Lyons *et al.*, 2013). Although this lack of effect could reflect structural defects of the axoneme similar to those seen in the *C. elegans ccpp-1* mutants (O'Hagan *et al.*, 2011), this could simply be due to restricted expression of *ccp1* in the zebrafish nervous system. In addition, the reported increase in glutamyl tubulin immunoreactivity in the *ccp1*-knockdown pronephric duct was restricted to the cytoplasm and not cilia associated (Lyons *et al.*, 2013). In *ccp1*-deficient embryos we did observe marked hydrocephalus, a phenotype often associated with ependymal cilia paralysis and impaired cerebrospinal fluid flow (Ibanez-Tallon *et al.*, 2004; Kramer-Zucker *et al.*, 2005). However, because the mouse *Ccp1/Pcd* mutant is known to exhibit a neuronal cell death phenotype, we used the apoptosis reporter annexin-GFP zebrafish transgenic (van Ham *et al.*, 2010) to examine the possibility that cell debris from dying neurons might obstruct the spinal canal and found that this was indeed the case. This result is a cautionary note in interpreting hydrocephalus purely as a ciliopathy,

since any physical obstruction of the spinal canal may produce hydrocephalus. Of the four *ccp* genes in zebrafish, we conclude that *ccp5* is specifically required to regulate axonemal tubulin glutamylation.

ccp-dependent regulation of cilia structure and function

Our work suggests that Ccp5 is normally active in cilia and is important for maintaining the appropriate level of axonemal tubulin glutamylation, since *ccp5* knockdown increased cilia tubulin glutamylation. Ccp5 may normally play a role in preventing formation of supernumerary glutamate chains that could compromise motility-associated functions of cilia microtubules. Hyperglutamylation has been shown to arrest motility of *Tetrahymena* cilia (Janke *et al.*, 2005) and induce structural defects in axonemal microtubules (O'Hagan *et al.*, 2011). Our results show that loss of *ccp5* induces hyperglutamylation in zebrafish pronephric cilia and reduces cilia beat coordination and beat amplitude without affecting beat frequency. This may reflect a preferential effect of hyperglutamylation on inner dynein arm activity, consistent with previously reported effects of TTLL deficiency on axonemal microtubule sliding and the role of inner dynein arms in regulating cilia waveform (Brokaw and Kamiya, 1987; Wood *et al.*, 2007; Suryavanshi *et al.*, 2010). We also observed microtubule doublet B-tubule gap defects, similar to *ttll* loss-of-function cilia (Pathak *et al.*, 2011), in a minority of cilia examined in *ccp5* morphants (unpublished data). Because cilia were uniformly hyperglutamylated but only a minority showed ultrastructural defects, it is likely the B-subfiber gaps are not a primary effect of hyperglutamylation but instead represent a late-stage breakdown of cilia structural integrity. Unlike mutations that completely disrupt cilia structure and show fully penetrant kidney cyst formation (Sun *et al.*, 2004; Sullivan-Brown *et al.*, 2008; Huang and Schier, 2009), kidney cyst formation in *ccp5*-knockdown embryos was only partially penetrant. This may reflect the fact that kidney cilia motility was not completely disrupted by *ccp5* knockdown but instead was disorganized and reduced in beat amplitude. We observed similar partial penetrance of kidney cyst formation in *ttll3/6*-gene knockdowns, which reduce tubulin glycylation and glutamylation (Pathak *et al.*, 2011) and produce a similar disorganized cilia beat pattern. Overall the results indicate that hypoglutamylation or hyperglutamylation of cilia tubulin disrupts cilia function and suggests that *ttll* ligases and *ccp* glutamylases act in concert to establish a functional "set-point" for tubulin modifications.

Ccp5, tubulin hyperglutamylation, and IFT proteins in cilia

The restoration of axonemal glutamylation and multicilia formation by *ccp5* knockdown in IFT protein–deficient zebrafish highlights the idea that tubulin glutamylation can have a dominant, positive effect on ciliogenesis. We chose to examine the effect of *ccp5* knockdown and hyperglutamylation on the *fleer*-mutant phenotype because we showed previously that zebrafish *fleer*-mutant single cilia lack tubulin glutamylation and that *fleer*-mutant multicilia fail to form (Pathak *et al.*, 2007). Because multiciliated cells contain more cilia (>20), it may be that the more severe ciliogenesis defect in these cells is due to more stringent IFT protein stoichiometric requirements for ciliogenesis. Although the exact mechanism of Fleer/Ift70 function in tubulin glutamylation is not known, there are several possibilities to account for loss of glutamylation in *fleer* mutants. Fleer may act to maintain the structural integrity of B-tubule protofilaments, the substrate for microtubule glutamylation (Kann *et al.*, 1995; Multigner *et al.*, 1996; Lechtreck and Geimer, 2000). Alternatively, it may serve as an IFT adaptor protein to facilitate axonemal transport of Ttll glutamylases and other essential axonemal proteins (Pathak *et al.*, 2007; Fan *et al.*, 2010; Taschner *et al.*, 2011, 2012; Zhao and Malicki, 2011). A new hypothesis based on our present work is that Fleer may act to suppress the activity of tubulin deglutamylases like Ccp5. Our finding that *fleer/ift70*-mutant cilia remain competent for glutamylation in *ccp5*-deficient embryos, as well as the finding that *C. elegans ccpp-1*-mutant cilia show enhanced glutamylation that is not reduced by mutation in the *fleer/ift70* orthologue Dyf-1 (O'Hagan *et al.*, 2011), supports this idea. Whatever the mechanism of Fleer activity may be, our results show a dominant effect of tubulin hyperglutamylation on multiciliogenesis not only in *fleer/ift70* mutants, but also in *ift88* morphants. Given that some maternal *fleer* mRNA may persist in zygotic mutants and that morpholino knockdown of *ift88* may not be complete, it is possible that some Fleer and Ift88 protein may be present and interact with higher affinity for hyperglutamylated axonemes. Nonetheless, our results raise the possibility that in some contexts, deficiencies of individual IFT proteins may be bypassed in ciliogenesis by enhanced recruitment of compensatory IFT proteins to forming cilia axonemes or possibly by enhanced activity of microtubule motor proteins in IFT transport. The identification and characterization of Ttll tubulin-modifying enzymes and Ccp deglutamylases should make it possible to determine the function of tubulin glutamylation in ciliogenesis.

MATERIALS AND METHODS

Zebrafish strains, maintenance, and genotyping

Wild-type TuAB, *fleer* mutant, transgenic CD-41-GFP, and transgenic UAS-annexin-V–yellow fluorescent protein lines were maintained according to standard procedures and used to obtain embryos for morpholino injections. Pigment formation in zebrafish larvae was suppressed by addition of (0.003%) 1-phenyl 2-thiourea to egg water after 20 and 24 hpf. The *fleer*^{ca1} mutant allele encodes a truncated 186–amino acid Fleer N-terminal peptide as opposed to the full-length Fleer protein of 651 amino acids (Leshchiner *et al.*, 2012). Embryos from in-crosses of *fleer*^{ca1} heterozygotes were genotyped by polymorphism of a simple sequence repeat in the vicinity of the *fleer* locus on zebrafish chromosome 3. Genomic DNA from tail clips of embryos was used to obtain DNA amplicons using the following PCR primers:

nZ1071F, CAGCTGCTACAGCAACCTGA

nZ1071R, GGACGCGGTATGTAACCTGT

Zebrafish *ccp* clones

Full- and partial-length cDNAs of zebrafish *ccp1* were amplified by reverse transcription (RT)-PCR based on their predicted sequence and cloned into pDONR 221 vector. Full-length clones of *ccp2* in pME18S-FL3 (BC146747) and *ccp5*/*agbl5* in pExpress-1 (BC080248) and a partial ccp6 EST (BC093361) in pME18S-FL3 were purchased from Open Biosystems (Huntsville, AL). Evolutionary analysis of ccp homologues is presented in Supplemental Figure S3 and was generated using clustalw (Chenna *et al.*, 2003) and drawtree in the Phylip 3.695 software package (Felsenstein, 1997).

Morpholino knockdown of *ccp* genes

Antisense morpholinos were designed to block specific splice donor sites within *ccp1*, *ccp2*, *ccp5*, and *ccp6* deglutamylase genes and purchased from Gene Tools (Philomath, OR). In the following morpholinos, the name of the targeted deglutamylase gene precedes the letter x, followed by the number of the specific target exon. The targeted splice site is underlined in the following sequences (5′–3′) of morpholinos:

Ccp1×5Mo: TTAAGAACACCAAAACTCACCGACA

Ccp2×2Mo: CCATACAGAAGTGGAGCTTACCTGA

Ccp5×5Mo: TCCTCTTAATGTGCAGATACCCGTT

Ccp5×8Mo: AAGTTTGACTCCTAGACGTACCTGT

Ccp6×3Mo: TTTACGTCCAAGTGCTTACCTGAGT

ift88(polaris)AUGMo: CTGGGACAAGATGCACATTCTCCAT (Kramer-Zucker *et al.*, 2005)

Control injections were performed using a heterologous inverse sense morpholino against *foxJ1a*:

foxJ1a conMo: CGTCCATTGTGTAAAAGTGTAACCA (Hellman *et al.*, 2010)

Morpholino oligonucleotides were dissolved in RNase-free water to a 2 mM stock concentration. For injections, morpholino dilutions were made in 100 mM KCl, 10 mM 4-(2-hydroxyethyl)-1-piperazineethanesulfonic acid (pH 7.4), and 0.1% phenol red. A Nanoliter 2000 microinjector (WPI Instruments, Sarasota, Fl) was used to inject 4.6-nl volumes in two- to four- cell embryos,. To detect morpholino-induced splicing defects upon injection of *ccp5×5*mo or *ccp5×8mo*, nested RT-PCR was performed on total RNA extracted from individual embryos using primers listed in Supplemental Table S1.

RNA in situ hybridization

Linearized DNA templates of *ccp1* and *ccp5* containing T7 promoter sites were obtained by restriction digestion of their clones with *Xma*1 and *Eco*R1, respectively. Linearized DNA templates of *ccp2* and *ccp6* cDNAs were generated from their pME18S-FL3 vectors by PCR, with the reverse primer engineered to contain the T7 promoter. Digoxigenin-labeled full-length antisense riboprobes of *ccp1*, *ccp2*, *ccp5*, and *ccp6* were synthesized by in vitro transcription using the T7 polymerase. Whole-mount RNA in situ hybridization was performed as described previously (Liu *et al.*, 2007; Thisse and Thisse, 2008). For imaging, the stained embryos were cleared in dimethyl formamide and mounted in 80% glycerol. Images were obtained using a Spot image digital camera mounted on a Leitz MZ12 stereomicroscope (Leica, Wetzlar, Germany) or Nikon E800 microscope (Nikon, Melville, NY).

Immunofluorescence: qualitative and quantitative analysis

Whole zebrafish larvae were fixed for immunolabeling in Dent's fixative (80% methanol, 20% dimethyl sulfoxide) at 4°C overnight. For visualization of pronephric cilia in control morphants, distension of the pronephric lumen was induced in the live larva by mechanical obstruction of their cloaca 1 h before fixation. The fixed specimens were rehydrated gradually and washed with phosphate-buffered saline (PBS) containing 0.5% Tween 20 (PBST) and blocked for 2 h with 5% normal goat serum before antibody labeling. For immunolabeling, the larvae were sequentially incubated with appropriate dilutions of each primary and secondary antibody overnight at 4°C. The dilutions of primary antibodies used were as follows: mAb GT335, 1:400 (Enzo Life Sciences, Plymouth Meeting, PA); mAb 6-11B-1, 1:800 (Sigma-Aldrich, St. Louis, MO); and Arl13b, 1:250 (gift from Z. Sun, Yale University). Immunoreactivity was detected using the secondary antibodies Alexa 546–conjugated goat anti rabbit (1:800), Alexa 546–conjugated goat anti-mouse, and Alexa 488–conjugated donkey anti-mouse (1:800). Immunolabeling with two mouse antibodies was performed as described earlier, with the first primary and secondary antibodies briefly fixed with 4% paraformaldehyde and their reactive sites blocked by sequential incubations in 10% unconjugated mouse serum and 5% unconjugated mouse Fab' fragments (Pathak *et al.*, 2007). Two-color confocal *Z*-series were acquired using sequential laser excitation under identical imaging conditions.

To analyze quantitatively the extent and intensities of glutamylated and acetylated tubulin in individual cilia, maximum intensity projection images were generated from deconvolved stacks using the Huygens Essential program (Scientific Volume Imaging, Hilversum, Netherlands) and saved in TIFF format. These maximum-intensity projections were viewed as composite color images using ImageJ (National Institutes of Health, Bethesda, MD), and lengths of lines drawn in separate red (glutamylated tubulin) and green (acetylated tubulin) channels were determined using the analyze function. The integrated pixel densities were similarly measured separately for red (glutamylated tubulin) and green (acetylated tubulin) channels in regions of interest drawn around individual cilia.

High-speed videomicroscopy analysis

The 54-hpf control and morpholino-injected, 1-phenyl 2-thiourea–treated embryos of wild-type TuAB or CD-41 GFP transgenic zebrafish were maintained alive and anesthetized in E3 egg water containing tricaine (1:25 dilution of 4.1% stock). The immobilized larvae were placed on 3% methyl cellulose, immersed in the anesthetic mix, and observed by Nomarski optics using a 40×/0.55 water immersion lens mounted on the Nikon E-800 microscope. Images of moving cilia in distended pronephric lumens (due to cystic phenotype or mechanical obstruction induced in the distal pronephros of controls) were obtained using the Dragonfly2 CCD camera (Point Grey Research, Richmond, Canada) at speeds between 235 and 245 frames/s. To obtain kymograms from sequential movie frames, the entire stack of 324 × 242 images in QuickTime movies (Apple, Cupertino, CA) were imported in ImageJ software, and the line function was used to slice the movie frames along a small plane orthogonal to the axis (near the center of cilium) of cilia selected for analysis. Beat amplitude information was assessed from the kymograms by determining the length of pixels between the extreme positions of the cilium and converted to a micrometer scale (1 µm = 2.7 pixels in a 324 × 242 tiff image). The beat frequency was assessed by measuring the number of peaks in the kymogram corresponding to a 1-s-long movie.

ACKNOWLEDGMENTS

We acknowledge Mohamed Adan for technical assistance, Tjakko Van Ham for the gift of UAS:annexin-V–GFP transgenic fish, and members of the Drummond lab for critical input to the manuscript. We also thank Carsten Janke for the GT335 antibody and Zhaoxia Sun for the Arl13b antibody. This work was supported by National Institutes of Health Grants K01DK078741 (N.P.), K08DK08272 and R03DK097443 (A.V.), and RO1DK053093 (I.A.D.).

REFERENCES

Bobinnec Y, Moudjou M, Fouquet JP, Desbruyeres E, Edde B, Bornens M (1998). Glutamylation of centriole and cytoplasmic tubulin in proliferating non-neuronal cells. Cell Motil Cytoskeleton 39, 223–232.

Bosch Grau M, Gonzalez Curto G, Rocha C, Magiera MM, Marques Sousa P, Giordano T, Spassky N, Janke C (2013). Tubulin glycylases and glutamylases have distinct functions in stabilization and motility of ependymal cilia. J Cell Biol 202, 441–451.

Brokaw CJ, Kamiya R (1987). Bending patterns of *Chlamydomonas* flagella: IV. Mutants with defects in inner and outer dynein arms indicate differences in dynein arm function. Cell Motil Cytoskeleton 8, 68–75.

Chenna R, Sugawara H, Koike T, Lopez R, Gibson TJ, Higgins DG, Thompson JD (2003). Multiple sequence alignment with the Clustal series of programs. Nucleic Acids Res 31, 3497–3500.

Edde B, Rossier J, Le Caer JP, Berwald-Netter Y, Koulakoff A, Gros F, Denoulet P (1991). A combination of posttranslational modifications is responsible for the production of neuronal alpha-tubulin heterogeneity. J Cell Biochem 46, 134–142.
Edde B, Rossier J, Le Caer JP, Desbruyeres E, Gros F, Denoulet P (1990). Posttranslational glutamylation of alpha-tubulin. Science 247, 83–85.
Fan ZC, Behal RH, Geimer S, Wang Z, Williamson SM, Zhang H, Cole DG, Qin H (2010). *Chlamydomonas* IFT70/CrDYF-1 is a core component of IFT particle complex B and is required for flagellar assembly. Mol Biol Cell 21, 2696–2706.
Felsenstein J (1997). An alternating least squares approach to inferring phylogenies from pairwise distances. Syst Biol 46, 101–111.
Fernandez-Gonzalez A, La Spada AR, Treadaway J, Higdon JC, Harris BS, Sidman RL, Morgan JI, Zuo J (2002). Purkinje cell degeneration (pcd) phenotypes caused by mutations in the axotomy-induced gene, Nna1. Science 295, 1904–1906.
Fouquet JP, Edde B, Kann ML, Wolff A, Desbruyeres E, Denoulet P (1994). Differential distribution of glutamylated tubulin during spermatogenesis in mammalian testis. Cell Motil Cytoskeleton 27, 49–58.
Hellman NE *et al*. (2010). The zebrafish foxj1a transcription factor regulates cilia function in response to injury and epithelial stretch. Proc Natl Acad Sci USA 107, 18499–18504.
Huang P, Schier AF (2009). Dampened Hedgehog signaling but normal Wnt signaling in zebrafish without cilia. Development 136, 3089–3098.
Huitorel P, White D, Fouquet JP, Kann ML, Cosson J, Gagnon C (2002). Differential distribution of glutamylated tubulin isoforms along the sea urchin sperm axoneme. Mol Reprod Dev 62, 139–148.
Ibanez-Tallon I, Pagenstecher A, Fliegauf M, Olbrich H, Kispert A, Ketelsen UP, North A, Heintz N, Omran H (2004). Dysfunction of axonemal dynein heavy chain Mdnah5 inhibits ependymal flow and reveals a novel mechanism for hydrocephalus formation. Hum Mol Genet 13, 2133–2141.
Ikegami K *et al*. (2007). Loss of alpha-tubulin polyglutamylation in ROSA22 mice is associated with abnormal targeting of KIF1A and modulated synaptic function. Proc Natl Acad Sci USA 104, 3213–3218.
Ikegami K, Mukai M, Tsuchida J, Heier RL, Macgregor GR, Setou M (2006). TTLL7 is a mammalian beta-tubulin polyglutamylase required for growth of MAP2-positive neurites. J Biol Chem 281, 30707–30716.
Ikegami K, Sato S, Nakamura K, Ostrowski LE, Setou M (2010). Tubulin polyglutamylation is essential for airway ciliary function through the regulation of beating asymmetry. Proc Natl Acad Sci USA 107, 10490–10495.
Janke C, Bulinski JC (2011). Post-translational regulation of the microtubule cytoskeleton: mechanisms and functions. Nat Rev Mol Cell Biol 12, 773–786.
Janke C *et al*. (2005). Tubulin polyglutamylase enzymes are members of the TTL domain protein family. Science 308, 1758–1762.
Kann ML, Prigent Y, Fouquet JP (1995). Differential distribution of glutamylated tubulin in the flagellum of mouse spermatozoa. Tissue Cell 27, 323–329.
Kann ML, Soues S, Levilliers N, Fouquet JP (2003). Glutamylated tubulin: diversity of expression and distribution of isoforms. Cell Motil Cytoskeleton 55, 14–25.
Kimura Y, Kurabe N, Ikegami K, Tsutsumi K, Konishi Y, Kaplan OI, Kunitomo H, Iino Y, Blacque OE, Setou M (2010). Identification of tubulin deglutamylase among *Caenorhabditis elegans* and mammalian cytosolic carboxypeptidases (CCPs). J Biol Chem 285, 22936–22941.
Kramer-Zucker AG, Olale F, Haycraft CJ, Yoder BK, Schier AF, Drummond IA (2005). Cilia-driven fluid flow in the zebrafish pronephros, brain and Kupffer's vesicle is required for normal organogenesis. Development 132, 1907–1921.
Kubo T, Yanagisawa HA, Yagi T, Hirono M, Kamiya R (2010). Tubulin polyglutamylation regulates axonemal motility by modulating activities of inner-arm dyneins. Curr Biol 20, 441–445.
Lacroix B, van Dijk J, Gold ND, Guizetti J, Aldrian-Herrada G, Rogowski K, Gerlich DW, Janke C (2010). Tubulin polyglutamylation stimulates spastin-mediated microtubule severing. J Cell Biol 189, 945–954.
Lechtreck KF, Geimer S (2000). Distribution of polyglutamylated tubulin in the flagellar apparatus of green flagellates. Cell Motil Cytoskeleton 47, 219–235.
Lee GS *et al*. (2013). Disruption of Ttll5/stamp gene (tubulin tyrosine ligase-like protein 5/SRC-1 and TIF2-associated modulatory protein gene) in male mice causes sperm malformation and infertility. J Biol Chem 288, 15167–15180.
Lee JE *et al*. (2012). CEP41 is mutated in Joubert syndrome and is required for tubulin glutamylation at the cilium. Nat Genet 44, 193–199.
Leshchiner I *et al*. (2012). Mutation mapping and identification by whole-genome sequencing. Genome Res 22, 1541–1548.
Liu Y, Pathak N, Kramer-Zucker A, Drummond IA (2007). Notch signaling controls the differentiation of transporting epithelia and multiciliated cells in the zebrafish pronephros. Development 134, 1111–1122.
Lyons PJ, Sapio MR, Fricker LD (2013). Zebrafish cytosolic carboxypeptidases 1 and 5 are essential for embryonic development. J Biol Chem 288, 30454–30462.
Mullen RJ, Eicher EM, Sidman RL (1976). Purkinje cell degeneration, a new neurological mutation in the mouse. Proc Natl Acad Sci USA 73, 208–212.
Multigner L, Pignot-Paintrand I, Saoudi Y, Job D, Plessmann U, Rudiger M, Weber K (1996). The A and B tubules of the outer doublets of sea urchin sperm axonemes are composed of different tubulin variants. Biochemistry 35, 10862–10871.
O'Hagan R, Piasecki BP, Silva M, Phirke P, Nguyen KC, Hall DH, Swoboda P, Barr MM (2011). The tubulin deglutamylase CCPP-1 regulates the function and stability of sensory cilia in *C. elegans*. Curr Biol 21, 1685–1694.
Pathak N, Austin CA, Drummond IA (2011). Tubulin tyrosine ligase-like genes ttll3 and ttll6 maintain zebrafish cilia structure and motility. J Biol Chem 286, 11685–11695.
Pathak N, Obara T, Mangos S, Liu Y, Drummond IA (2007). The zebrafish fleer gene encodes an essential regulator of cilia tubulin polyglutamylation. Mol Biol Cell 18, 4353–4364.
Rogowski K *et al*. (2010). A family of protein-deglutamylating enzymes associated with neurodegeneration. Cell 143, 564–578.
Spiliotis ET, Hunt SJ, Hu Q, Kinoshita M, Nelson WJ (2008). Epithelial polarity requires septin coupling of vesicle transport to polyglutamylated microtubules. J Cell Biol 180, 295–303.
Sullivan-Brown J, Schottenfeld J, Okabe N, Hostetter CL, Serluca FC, Thiberge SY, Burdine RD (2008). Zebrafish mutations affecting cilia motility share similar cystic phenotypes and suggest a mechanism of cyst formation that differs from pkd2 morphants. Dev Biol 314, 261–275.
Sun Z, Amsterdam A, Pazour GJ, Cole DG, Miller MS, Hopkins N (2004). A genetic screen in zebrafish identifies cilia genes as a principal cause of cystic kidney. Development 131, 4085–4093.
Suryavanshi S *et al*. (2010). Tubulin glutamylation regulates ciliary motility by altering inner dynein arm activity. Curr Biol 20, 435–440.
Taschner M, Bhogaraju S, Lorentzen E (2012). Architecture and function of IFT complex proteins in ciliogenesis. Differentiation 83, S12–S22.
Taschner M, Bhogaraju S, Vetter M, Morawetz M, Lorentzen E (2011). Biochemical mapping of interactions within the intraflagellar transport (IFT) B core complex: IFT52 binds directly to four other IFT-B subunits. J Biol Chem 286, 26344–26352.
Thisse C, Thisse B (2008). High-resolution in situ hybridization to whole-mount zebrafish embryos. Nat Protoc 3, 59–69.
Tsujikawa M, Malicki J (2004). Intraflagellar transport genes are essential for differentiation and survival of vertebrate sensory neurons. Neuron 42, 703–716.
van Dijk J, Rogowski K, Miro J, Lacroix B, Edde B, Janke C (2007). A targeted multienzyme mechanism for selective microtubule polyglutamylation. Mol Cell 26, 437–448.
van Ham TJ, Mapes J, Kokel D, Peterson RT (2010). Live imaging of apoptotic cells in zebrafish. FASEB J 24, 4336–4342.
Verhey KJ, Gaertig J (2007). The tubulin code. Cell Cycle 6, 2152–2160.
Vogel P, Hansen G, Fontenot G, Read R (2010). Tubulin tyrosine ligase-like 1 deficiency results in chronic rhinosinusitis and abnormal development of spermatid flagella in mice. Vet Pathol 47, 703–712.
Wood CR, Hard R, Hennessey TM (2007). Targeted gene disruption of dynein heavy chain 7 of *Tetrahymena thermophila* results in altered ciliary waveform and reduced swim speed. J Cell Sci 120, 3075–3085.
Zhao C, Malicki J (2011). Nephrocystins and MKS proteins interact with IFT particle and facilitate transport of selected ciliary cargos. EMBO J 30, 2532–2544.